

Tetrafluoroborate-Monofluorophosphate $(\text{NH}_4)_3[\text{PO}_3\text{F}][\text{BF}_4]$: First Member of Oxyfluoride with B–F and P–F Bonds

Haotian Qiu, Wenbing Cai, Zhihua Yang, Yanli Liu, Miriding Mutailipu,* and Shilie Pan*

Cite This: *ACS Org. Inorg. Au* 2021, 1, 6–10

Read Online

ACCESS |



Metrics & More

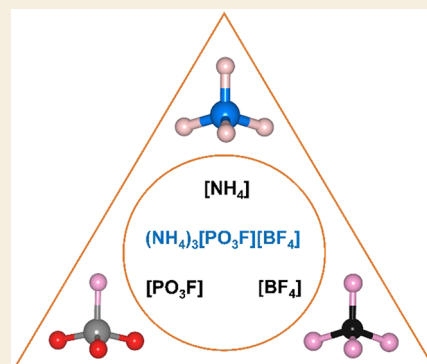


Article Recommendations



Supporting Information

ABSTRACT: Inspired by the strategy of fluorine introduction in borates and phosphates, the inorganic oxyfluoride $(\text{NH}_4)_3[\text{PO}_3\text{F}][\text{BF}_4]$ with B–F and P–F bonds has been characterized as the first fluoroborate-fluorophosphate. The International Union of Pure and Applied Chemistry (IUPAC) name for $(\text{NH}_4)_3[\text{PO}_3\text{F}][\text{BF}_4]$ should be ammonium tetrafluoroborate-monofluorophosphate according to the structure characteristics. The existence and coordination of fluorine in $(\text{NH}_4)_3[\text{PO}_3\text{F}][\text{BF}_4]$ were confirmed by several approaches, including single-crystal structure analysis; bond valence analysis; and X-ray energy dispersive, infrared spectrum, and also nuclear magnetic resonance spectroscopy. This work is of great significance to enrich the solid-state chemistry of borates and phosphates and also open a new branch of mixed anion compound with fluoroborate-fluorophosphates.



KEYWORDS: Oxyfluoride, fluoroborate-fluorophosphate, mixed anions, borates, phosphates

Within the past decade, there has been an increasing interest in solids with mixed anions that can improve the finding of new novel structures and materials.^{1–4} The multiple or mixed anion compound is a phase that contains more than one type of anion, which shows better performance and rich structural chemistry when compared with its homoanionic compounds.¹

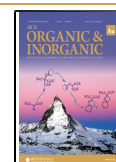
Oxyfluoride (or oxide-fluoride) is an important branch of mixed anion compounds, and therefore, considerable efforts have been made to find new oxyfluorides and also to understand the crucial roles of multiple anions on property modification.^{1,2,5} In recent years, oxyfluorides with different types of fluorinated $[\text{MO}_{m-n}\text{F}_n]$ ($M = \text{B}, \text{P}, \text{S}, \text{Si}; m = 4, 6; n = 1–3$, etc.) units have been designed using the strategy of fluorine introduction in oxides, which has expanded the solid-state chemistry with newly developed branches and systems like fluorooxoborates,^{6–16} fluorophosphates,^{17,18} fluorooxosilicates,^{19,20} and fluorooxosulfates.^{21,22} The fluorinated units in these oxyfluorides have an indispensable role for the improved symmetry, enlarged energy gap, and enhanced polarizability anisotropy, which can be regarded as new optical-active units for regulating the microstructures and optical properties. Fluorooxoborates tend to form layered configurations, which can be verified by the increased proportion of fluorooxoborates in two-dimensional layered structures (53.33%) when compared with borates (10.26%) without fluorinated $[\text{BO}_{4-n}\text{F}_n]$ ($n = 1–3$) units.³ Also, unlike $[\text{PO}_4]$ units in phosphates that can produce a high degree of polymerization,^{23–25} fluorinated $[\text{PO}_3\text{F}]$ and $[\text{PO}_2\text{F}_2]$ units are generally in isolated form (a few $[\text{PO}_3\text{F}]$ units can form

$[\text{P}_2\text{O}_5\text{F}_2]$ dimers),^{17,18} reducing the dimension of fluorophosphates to zero dimensional structure.

The combination of different anion groups is also a common design strategy for synthesizing new mixed anion compounds. With respect to the combination of borates and phosphates, there are two types of compounds with B–O and P–O bonds according to the classification proposed by Kniep et al.:²⁶ (i) borophosphates and (ii) borate-phosphates, in which the B–O units link with P–O units for the former branch, whereas the two different anion groups are in isolated configuration in the latter. The number of borate-phosphates is extremely limited when compared with borophosphates.²⁶ In principle, the introduction of fluorine in above two systems can form more oxyfluorides, like fluoroborophosphates, borofluorophosphates, fluorooxoborate-fluorophosphates, and fluoroborate-fluorophosphates. But there are only a few cases for fluoroborophosphates and borofluorophosphates,^{27–29} and no related inorganic compounds are reported in fluorooxoborate-fluorophosphates and fluoroborate-fluorophosphates (with both B–F and P–F bonds). Herein, by combining fluoroborates and fluorophosphates, $(\text{NH}_4)_3[\text{PO}_3\text{F}][\text{BF}_4]$, the first inorganic oxyfluoride with both B–F and P–F bonds has

Received: July 15, 2021

Published: August 4, 2021



been synthesized, which is the first case in fluoroborate-fluorophosphate system.

Single crystals of $(\text{NH}_4)_3[\text{PO}_3\text{F}][\text{BF}_4]$ were grown via liquid phase neutralization at room temperature. A mixture of $\text{Na}_2\text{PO}_3\text{F}$, $(\text{NH}_4)\text{HF}_2$ and H_3BO_3 with the molar ratio of 1:3:1 was dissolved in 50 mL deionized water and stirred to make it completely clear. Then, colorless $(\text{NH}_4)_3[\text{PO}_3\text{F}][\text{BF}_4]$ crystals were obtained at the bottom of beaker after several days with the yield of about 70%. Single-crystal X-ray diffraction analysis and Rietveld refinement were used to determine the crystal structure and confirm the purity of as-prepared polycrystalline samples. The fitted profile matches well with the experimental powder X-ray diffraction patterns, having the acceptable R values of $R_p = 0.0606$ and $R_{wp} = 0.0848$ (Figures S1 and S2 in the Supporting Information (SI)). According to the structure characteristics of $(\text{NH}_4)_3[\text{PO}_3\text{F}][\text{BF}_4]$ ($[\text{PO}_3\text{F}]$ and $[\text{BF}_4]$ are in isolated configuration), the International Union of Pure and Applied Chemistry (IUPAC) name³⁰ for $(\text{NH}_4)_3[\text{PO}_3\text{F}][\text{BF}_4]$ should be ammonium tetrafluoroborate-monofluorophosphate. $(\text{NH}_4)_3[\text{PO}_3\text{F}][\text{BF}_4]$ crystallizes in the monoclinic crystal system with the space group $P2_1/m$ (see Table S1 in the SI for details). As shown in Figure 1, the structure of $(\text{NH}_4)_3[\text{PO}_3\text{F}][\text{BF}_4]$

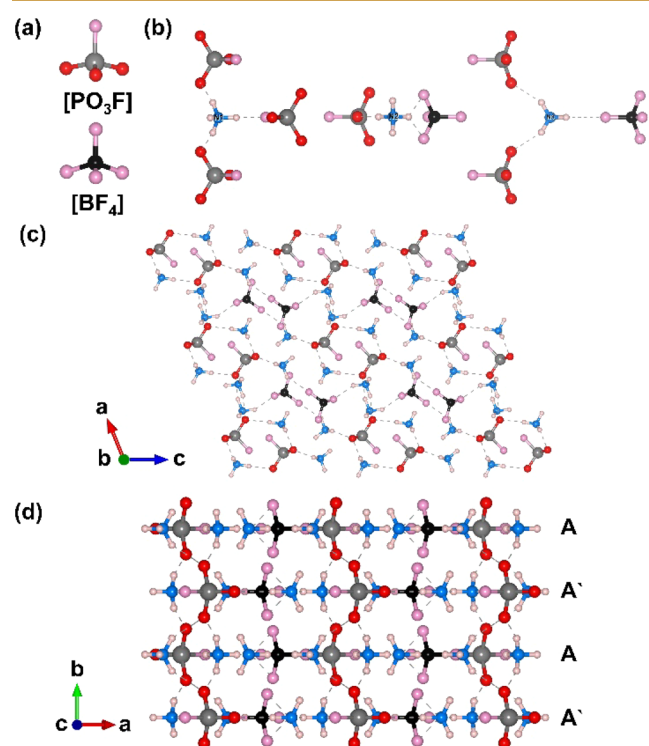


Figure 1. (a) Two types of anionic units in $(\text{NH}_4)_3[\text{PO}_3\text{F}][\text{BF}_4]$. (b) Coordination environment of three crystallographically independent $[\text{NH}_4]$ units. (c, d) Crystal structure of $(\text{NH}_4)_3[\text{PO}_3\text{F}][\text{BF}_4]$ along b and c axes, respectively. Atomic models: N (blue balls), P (gray balls), B (black balls), H (baby pink balls), O (red balls), and F (pink balls).

$[\text{BF}_4]$ is composed of three isolated units, that is, $[\text{NH}_4]$, $[\text{PO}_3\text{F}]$, and $[\text{BF}_4]$ units. In an asymmetric unit, there are three crystallographically independent $[\text{NH}_4]$ ammonium cations, one $[\text{PO}_3\text{F}]$ monofluorophosphate anion, and one $[\text{BF}_4]$ perfluorinated anion (Tables S1–S7 in the SI). It should be noted that all the $[\text{PO}_3\text{F}]$ and $[\text{BF}_4]$ units are in an isolated configuration without any connection and thus

$(\text{NH}_4)_3[\text{PO}_3\text{F}][\text{BF}_4]$ can be classified as fluoroborate-fluorophosphates, which is the first case in this family. The P–O, P–F, and B–F bond lengths are in the region of 1.471–1.478, 1.590, and 1.385–1.396 Å, respectively, which show a good match with other reported fluoroxyborates and fluorophosphates.^{6–18} The reasonable bond lengths also give the acceptable bond valence sum calculations and oxidation states of related atoms (Table S2 in the SI). The hydrogen bonds from $[\text{NH}_4]$ units in $(\text{NH}_4)_3[\text{PO}_3\text{F}][\text{BF}_4]$ link the whole structure, that is N–H···O bonds for $[\text{PO}_3\text{F}]$ and N–H···F bonds for $[\text{BF}_4]$ units, respectively. For three ammonium cations with different crystallographic positions (Figure 1b), $[\text{N}(1)\text{H}_4]$, $[\text{N}(2)\text{H}_4]$, and $[\text{N}(3)\text{H}_4]$ link with three $[\text{PO}_3\text{F}]$ units, one $[\text{PO}_3\text{F}]$ and one $[\text{BF}_4]$ unit, and two $[\text{PO}_3\text{F}]$ and one $[\text{BF}_4]$ units with N–H···O and N–H···F bonds, respectively. Along the c axis (Figure 1d), two alternate pseudolayers composed of $[\text{NH}_4]$, $[\text{PO}_3\text{F}]$, and $[\text{BF}_4]$ units further stack in the –AA'AA'– sequence, of which the interlayer force only comes from N–H···O bonds, whereas the intramural force originates from N–H···O and N–H···F bonds.³¹

The existence and coordination of fluorine in $(\text{NH}_4)_3[\text{PO}_3\text{F}][\text{BF}_4]$ were confirmed by several approaches: (1) **Single-crystal structure analysis and bond valence model.** Based on the single-crystal structure analysis, the final solved structure reveals that the related bond lengths and bond angles in $[\text{PO}_3\text{F}]$ and $[\text{BF}_4]$ of $(\text{NH}_4)_3[\text{PO}_3\text{F}][\text{BF}_4]$ are consistent with those of reported monofluorophosphates and tetrafluoroborates,^{6–18} giving preliminary confirmation of well-ordered O/F anions in $(\text{NH}_4)_3[\text{PO}_3\text{F}][\text{BF}_4]$. According to the results of bond valence calculations (BVS) (Table S1 in the SI), the valences of P (5.31), B (3.00), O (1.81–1.82), and F (0.73–0.87) are also reasonable, which verifies that the assignment of O and F atoms. (2) **X-ray energy dispersive and infrared spectrum.** According to the results of EDS (Figure S3 in the SI), the existence of P, B, and F was confirmed. In addition, as shown in Figure S4 in the SI, the IR spectrum of $(\text{NH}_4)_3[\text{PO}_3\text{F}][\text{BF}_4]$ shows that the characteristic vibrations at 2919–3363 cm^{-1} can be assigned to the stretching of $[\text{NH}_4]$.^{9,32} The asymmetrical, symmetrical stretching and scissoring vibrations of P–O bonds are observed at 1069–1124, 1022, 539 cm^{-1} , respectively. Particularly, the P–F stretching vibrations are observed at 760 cm^{-1} .¹⁷ Whereas, the peaks at 995 and 521 cm^{-1} are assigned to the stretching and scissoring vibrations of $[\text{BF}_4]$, respectively.^{33–35} All the assignments marked in Figure S4 are all based on the infrared spectra of related fluorophosphates, tetrafluoroborates and on other related literature data. (3) **Nuclear magnetic resonance spectroscopy.** The ^{19}F and $^{11}\text{B}/^{31}\text{P}$ magic-angle spinning (MAS) NMR spectra of $(\text{NH}_4)_3[\text{PO}_3\text{F}][\text{BF}_4]$ are visualized in Figure 2, in which the spinning sidebands are marked by asterisks. From the ^{19}F MAS NMR spectrum (Figure 2c), the signals at –71.43 and –73.24 ppm are assigned to F in $[\text{PO}_3\text{F}]$ units, whereas the signals at –140.26 and –146.49 ppm are assigned to F in $[\text{BF}_4]$ units, which are consistent with previous reports.^{34,36} For the ^{31}P MAS NMR spectrum (Figure 2a), two signals at –2.43 and 1.79 ppm of ^{31}P NMR are close to the chemical shifts in $\text{NaNH}_4\text{PO}_3\text{F}\cdot\text{H}_2\text{O}$ with similar $[\text{PO}_3\text{F}]$ tetrahedra.³² The $^{11}\text{B}\{^{19}\text{F}\}$ and $^{31}\text{P}\{^{19}\text{F}\}$ REDOR tests were carried out to establish the B–F and P–F bonds for tetrahedral $[\text{BF}_4]$ and $[\text{PO}_3\text{F}]$ units and the obtained different spectra are shown in Figures 2d and e, indicating that there are tetrahedral

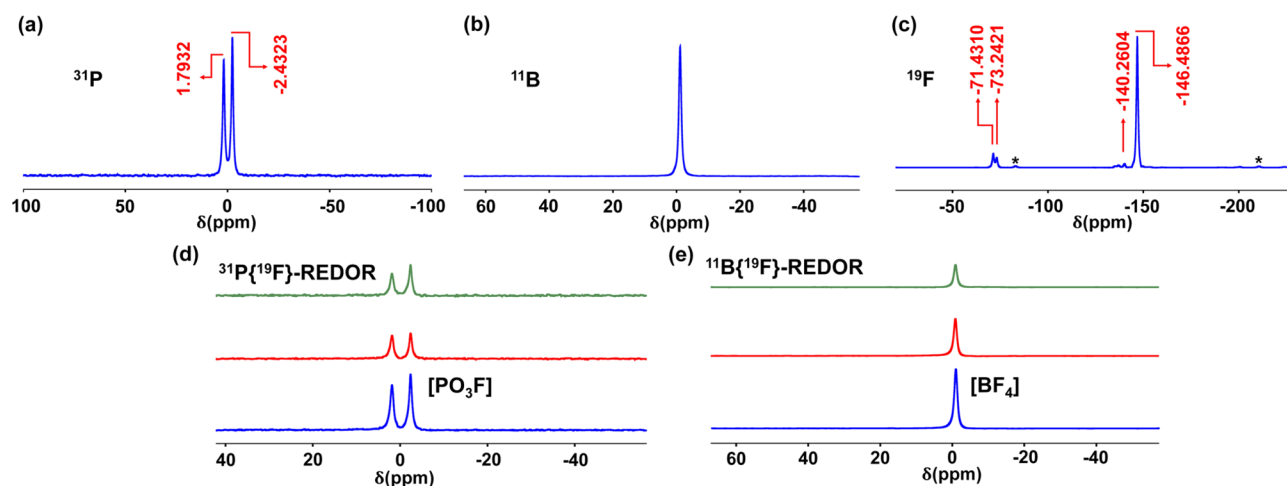


Figure 2. (a) ^{31}P , (b) ^{11}B , (c) ^{19}F , (d) $^{31}\text{P}\{^{19}\text{F}\}$ REDOR MAS, and (e) $^{11}\text{B}\{^{19}\text{F}\}$ REDOR MAS NMR of $(\text{NH}_4)_3[\text{PO}_3\text{F}][\text{BF}_4]$.

coordinated B and P nuclei with B–F and P–F bonds in the structure of $(\text{NH}_4)_3[\text{PO}_3\text{F}][\text{BF}_4]$. The $^{31}\text{P}\{^{19}\text{F}\}$ REDOR NMR experiment (Figure 2d) shows that two sharp peaks are typical for monofluorophosphates and provides powerful evidence for the existence of $[\text{PO}_3\text{F}]$ units in title compound.^{37,38} For the ^{11}B MAS NMR spectrum (Figure 2b), tetrahedral coordinated B atoms with high local electronic symmetry can be determined by the single signal near 0 ppm. In addition, the existence of B–F bonds is also confirmed by the $^{11}\text{B}\{^{19}\text{F}\}$ REDOR NMR experiment (Figure 2e), illustrating that $(\text{NH}_4)_3[\text{PO}_3\text{F}][\text{BF}_4]$ possesses tetrahedral $[\text{BF}_4]$ units with the chemical shift close to 0 ppm.³⁶ Based on the above analysis, the existences of $[\text{PO}_3\text{F}]$ and $[\text{BF}_4]$ tetrahedra are further confirmed.

In order to study the thermal stability of $(\text{NH}_4)_3[\text{PO}_3\text{F}][\text{BF}_4]$, thermogravimetric analysis (TG) and differential scanning calorimetry (DSC) were performed. As shown in Figure S5 in the SI, $(\text{NH}_4)_3[\text{PO}_3\text{F}][\text{BF}_4]$ releases three NH_3 , one HF, and one BF_3 gas molecule at about 195, 208, and 304 °C, respectively, as indicated on the DSC curve. The mass loss (26.84%) of the first stage comes from NH_3 and HF, whereas the mass loss (28.19%) of the latter curve is from BF_3 , which is consistent with the theoretical values of 29.75 and 28.38%, respectively. The UV–vis–NIR diffuse reflectance spectrum (Figure S6 in the SI) indicates that the cutoff edge of $(\text{NH}_4)_3[\text{PO}_3\text{F}][\text{BF}_4]$ is below 190 nm, proving that $(\text{NH}_4)_3[\text{PO}_3\text{F}][\text{BF}_4]$ crystal possesses a high potential of deep-UV optical crystal. Even at 190 nm, its reflectance rate is nearly 74%, which is comparable or shorter to most of alkali and alkaline earth metal fluorooxoborates and fluorophosphates.^{6–18} The short cutoff edge of $(\text{NH}_4)_3[\text{PO}_3\text{F}][\text{BF}_4]$ can be explained by the following structural aspects: (1) The constituents in $(\text{NH}_4)_3[\text{PO}_3\text{F}][\text{BF}_4]$, that is, N, P, B, O, F, and H atoms, effectively inhibit the unfavorable $d-d$ and $f-f$ electronic transitions and broaden the transparency window into deep-UV spectral region. (2) The anionic framework of $(\text{NH}_4)_3[\text{PO}_3\text{F}][\text{BF}_4]$ is exclusively constructed by non- π -conjugated tetrahedra, $[\text{BF}_4]$ and $[\text{PO}_3\text{F}]$ units, which is beneficial for a wider band gap and shorter cutoff edge. Furthermore, the electronic structures of $(\text{NH}_4)_3[\text{PO}_3\text{F}][\text{BF}_4]$ based on density functional theory (DFT) were calculated and analyzed. As shown in Figure 3a, $(\text{NH}_4)_3[\text{PO}_3\text{F}][\text{BF}_4]$ is an indirect band gap compound with the value of 5.02 eV (GGA). In order to analyze the determinant of the band gap, the total

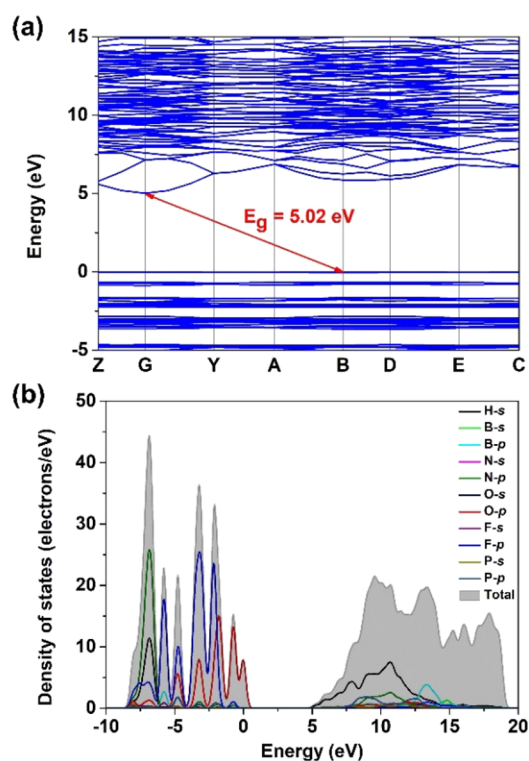


Figure 3. (a) Electron band structure of $(\text{NH}_4)_3[\text{PO}_3\text{F}][\text{BF}_4]$. (b) Calculated projected density of states in $(\text{NH}_4)_3[\text{PO}_3\text{F}][\text{BF}_4]$.

and partial densities of states (DOS and PDOS) of $(\text{NH}_4)_3[\text{PO}_3\text{F}][\text{BF}_4]$ are shown in Figure 3b. Obviously, near the Fermi level, the F $2p$, O $2p$, and N $2p$ orbitals play a decisive role on the top of the valence band. The bottom of the conduction band is mainly composed of P $3s$ and H $1s$ orbitals. Accordingly, the $[\text{NH}_4]$ and $[\text{PO}_3\text{F}]$ units have a major impact on the band gap. In addition, the calculated birefringence is 0.012@1064 nm by the first-principles calculations, and the birefringence dispersion curve is plotted in Figure S7 in the SI. Such a small birefringence can be accepted since the anionic framework of $(\text{NH}_4)_3[\text{PO}_3\text{F}][\text{BF}_4]$ is exclusively constructed by non- π -conjugated tetrahedra with relatively small optical anisotropy and they are also not in preferential arrangement.

In summary, a novel inorganic oxyfluoride $(\text{NH}_4)_3[\text{PO}_3\text{F}][\text{BF}_4]$ has been synthesized via liquid phase neutralization at

room temperature. It is the first case that contains B–F and P–F bonds in oxyfluorides, and the anionic framework is exclusively constructed by two isolated tetrahedra, that is, $[\text{PO}_3\text{F}]$ and $[\text{BF}_4]$. Thus, $(\text{NH}_4)_3[\text{PO}_3\text{F}][\text{BF}_4]$ is also the first compound belonging to the classification of fluoroborate-fluorophosphates. The $^{11}\text{B}\{^{19}\text{F}\}$ and $^{31}\text{P}\{^{19}\text{F}\}$ REDOR tests confirm the existence of tetrahedral coordinated B and P nuclei with B–F and P–F bonds in the structure of $(\text{NH}_4)_3[\text{PO}_3\text{F}][\text{BF}_4]$.

■ ASSOCIATED CONTENT

SI Supporting Information

The Supporting Information is available free of charge at <https://pubs.acs.org/doi/10.1021/acsorginorgau.1c00018>.

Experimental section, crystal data and structure refinement, atomic coordinates equivalent isotropic displacement parameters, bond valence sum, anisotropic displacement parameters, bond lengths, bond angles, hydrogen bonds, hydrogen atom coordinates, the experimental/calculated PXRD patterns, rietveld refinement of the powder XRD profile, the energy-dispersive X-ray spectroscopy, the IR spectrum, the TG-DSC curves, the UV–vis–NIR diffuse reflectance spectrum, and the birefringence curve for $(\text{NH}_4)_3[\text{PO}_3\text{F}][\text{BF}_4]$ (PDF)

Accession Codes

CCDC 2094843 contains the supplementary crystallographic data for this paper. These data can be obtained free of charge via www.ccdc.cam.ac.uk/data_request/cif, or by emailing data_request@ccdc.cam.ac.uk, or by contacting The Cambridge Crystallographic Data Centre, 12 Union Road, Cambridge CB2 1EZ, UK; fax: +44 1223 336033.

■ AUTHOR INFORMATION

Corresponding Authors

Shilie Pan – CAS Key Laboratory of Functional Materials and Devices for Special Environments, Xinjiang Technical Institute of Physics & Chemistry, CAS; Xinjiang Key Laboratory of Electronic Information Materials and Devices, Urumqi 830011, China; Center of Materials Science and Optoelectronics Engineering, University of Chinese Academy of Sciences, Beijing 100049, China; orcid.org/0000-0003-4521-4507; Email: slpan@ms.xjb.ac.cn

Miriding Mutailipu – CAS Key Laboratory of Functional Materials and Devices for Special Environments, Xinjiang Technical Institute of Physics & Chemistry, CAS; Xinjiang Key Laboratory of Electronic Information Materials and Devices, Urumqi 830011, China; Center of Materials Science and Optoelectronics Engineering, University of Chinese Academy of Sciences, Beijing 100049, China; orcid.org/0000-0002-1331-0185; Email: miriding@ms.xjb.ac.cn

Authors

Haotian Qiu – CAS Key Laboratory of Functional Materials and Devices for Special Environments, Xinjiang Technical Institute of Physics & Chemistry, CAS; Xinjiang Key Laboratory of Electronic Information Materials and Devices, Urumqi 830011, China; Center of Materials Science and Optoelectronics Engineering, University of Chinese Academy of Sciences, Beijing 100049, China

Wenbing Cai – CAS Key Laboratory of Functional Materials and Devices for Special Environments, Xinjiang Technical Institute of Physics & Chemistry, CAS; Xinjiang Key Laboratory of Electronic Information Materials and Devices, Urumqi 830011, China

Zhihua Yang – CAS Key Laboratory of Functional Materials and Devices for Special Environments, Xinjiang Technical Institute of Physics & Chemistry, CAS; Xinjiang Key Laboratory of Electronic Information Materials and Devices, Urumqi 830011, China; Center of Materials Science and Optoelectronics Engineering, University of Chinese Academy of Sciences, Beijing 100049, China; orcid.org/0000-0001-9214-3612

Yanli Liu – College of Materials Science and Engineering, Hunan University, Changsha 410004, China

Complete contact information is available at: <https://pubs.acs.org/doi/10.1021/acsorginorgau.1c00018>

Notes

The authors declare no competing financial interest.

■ ACKNOWLEDGMENTS

The authors gratefully acknowledge the National Natural Science Foundation of China (51972336), Xinjiang Tianshan Youth Program-Outstanding Young Science and Technology Talents (2019Q026), National Key Research Project (2016YFB0402104), the International Partnership Program of CAS (1A1365KYSB20200008), and the Western Light Foundation of CAS (Y92S191301).

■ REFERENCES

- (1) Kageyama, H.; Hayashi, K.; Maeda, K.; Attfield, J. P.; Hiroi, Z.; Rondinelli, J. M.; Poeppelmeier, K. R. Expanding Frontiers in Materials Chemistry and Physics with Multiple Anions. *Nat. Commun.* **2018**, *9*, 1–15.
- (2) Harada, J. K.; Charles, N.; Poeppelmeier, K. R.; Rondinelli, J. M. Heteroanionic Materials by Design: Progress Toward Targeted Properties. *Adv. Mater.* **2019**, *31*, 1805295.
- (3) Mutailipu, M.; Poeppelmeier, K. R.; Pan, S. L. Borates: A Rich Source for Optical Materials. *Chem. Rev.* **2021**, *121*, 1130–1202.
- (4) Charles, N.; Saballos, R. J.; Rondinelli, J. M. Structural Diversity from Anion Order in Heteroanionic Materials. *Chem. Mater.* **2018**, *30*, 3528–3537.
- (5) Bai, S.; Wang, D.; Liu, H. K.; Wang, Y. Recent Advances of Oxyfluorides for Nonlinear Optical Applications. *Inorg. Chem. Front.* **2021**, *8*, 1637–1654.
- (6) Mutailipu, M.; Zhang, M.; Yang, Z. H.; Pan, S. L. Targeting the Next Generation of Deep-Ultraviolet Nonlinear Optical Materials: Expanding from Borates to Borate Fluorides to Fluorooxoborates. *Acc. Chem. Res.* **2019**, *52*, 791–801.
- (7) Pilz, T.; Jansen, M. $\text{Li}_2\text{B}_6\text{O}_9\text{F}_2$, A New Acentric Fluorooxoborate. *Z. Anorg. Allg. Chem.* **2011**, *637*, 2148–2152.
- (8) Pilz, T.; Nuss, H.; Jansen, M. $\text{Li}_2\text{B}_3\text{O}_4\text{F}_3$, A New Lithium-rich Fluorooxoborate. *J. Solid State Chem.* **2012**, *186*, 104–108.
- (9) Shi, G. Q.; Wang, Y.; Zhang, F. F.; Zhang, B. B.; Yang, Z. H.; Hou, X. L.; Pan, S. L.; Poeppelmeier, K. R. Finding the Next Deep-Ultraviolet Nonlinear Optical Material: $\text{NH}_4\text{B}_4\text{O}_6\text{F}$. *J. Am. Chem. Soc.* **2017**, *139*, 10645–10648.
- (10) Wang, X. F.; Wang, Y.; Zhang, B. B.; Zhang, F. F.; Yang, Z. H.; Pan, S. L. $\text{CsB}_4\text{O}_6\text{F}$: A Congruent-Melting Deep-Ultraviolet Nonlinear Optical Material by Combining Superior Functional Units. *Angew. Chem., Int. Ed.* **2017**, *56*, 14119–14123.
- (11) Jantz, S. G.; Dialer, M.; Bayarjargal, L.; Winkler, B.; van Wüllen, L.; Pielhofer, F.; Brgoch, J.; Wehrich, R.; Höpfe, H. A. $\text{Sn}[\text{B}_2\text{O}_3\text{F}_2]$

The First Tin Fluorooxoborate as Possible NLO Material. *Adv. Opt. Mater.* **2018**, *6*, 1800497.

(12) Jantz, S. G.; Pielhofer, F.; van Wüllen, L.; Wehrich, R.; Schäfer, M. J.; Höpfe, H. The First Alkaline-Earth Fluorooxoborate $\text{Ba}[\text{B}_4\text{O}_6\text{F}_2]$ -Characterisation and Doping with Eu^{2+} . *Chem. - Eur. J.* **2018**, *24*, 443–450.

(13) Xia, M.; Li, F. M.; Mutailipu, M.; Han, S. J.; Yang, Z. H.; Pan, S. L. Discovery of First Magnesium Fluorooxoborate with Stable Fluorine Terminated Framework for Deep-UV Nonlinear Optical Application. *Angew. Chem., Int. Ed.* **2021**, *60*, 14650–14656.

(14) Bai, Z. Y.; Liu, L. H.; Wang, D. M.; Hu, C. L.; Lin, Z. B. To Improve the Key Properties of Nonlinear Optical Crystals Assembled with Tetrahedral Functional Building Units. *Chem. Sci.* **2021**, *12*, 4014–4020.

(15) Mutailipu, M.; Zhang, M.; Zhang, B. B.; Wang, L. Y.; Yang, Z. H.; Zhou, X.; Pan, S. L. $\text{SrB}_3\text{O}_7\text{F}_3$ Functionalized with $[\text{B}_3\text{O}_6\text{F}_3]^{6-}$ Chromophores: Accelerating the Rational Design of Deep-Ultraviolet Nonlinear Optical Materials. *Angew. Chem., Int. Ed.* **2018**, *57*, 6095–6099.

(16) Jin, C. C.; Shi, X. P.; Zeng, H.; Han, S. J.; Chen, Z.; Yang, Z. H.; Mutailipu, M.; Pan, S. L. Hydroxyfluorooxoborate $\text{Na}[\text{B}_3\text{O}_3\text{F}_2(\text{OH})_2] \cdot [\text{B}(\text{OH})_3]$: Optimizing the Optical Anisotropy with Heteroanionic Units for Deep Ultraviolet Birefringent Crystals. *Angew. Chem., Int. Ed.* **2021**, DOI: 10.1002/anie.202107291.

(17) Xiong, L.; Chen, J.; Lu, J.; Pan, C. Y.; Wu, L. M. Monofluorophosphates: A New Source of Deep-Ultraviolet Nonlinear Optical Materials. *Chem. Mater.* **2018**, *30*, 7823–7830.

(18) Zhang, B. B.; Han, G. P.; Wang, Y.; Chen, X. L.; Yang, Z. H.; Pan, S. L. Expanding Frontiers of Ultraviolet Nonlinear Optical Materials with Fluorophosphates. *Chem. Mater.* **2018**, *30*, 5397–5403.

(19) Han, G. P.; Lei, B. H.; Yang, Z. H.; Wang, Y.; Pan, S. L. A Fluorooxosilicate with Unprecedented SiO_2F_4 Species. *Angew. Chem., Int. Ed.* **2018**, *57*, 9828–9832.

(20) Ding, Q. R.; Liu, X. M.; Zhao, S. G.; Wang, Y. S.; Li, Y. Q.; Li, L. N.; Liu, S.; Lin, Z. S.; Hong, M. C.; Luo, J. H. Designing a Deep-UV Nonlinear Optical Fluorooxosilicophosphate. *J. Am. Chem. Soc.* **2020**, *142*, 6472–6476.

(21) Luo, M.; Lin, C.; Lin, D.; Ye, N. Rational Design of the Metal-Free $\text{KBe}_2\text{BO}_3\text{F}_2$ (KBBF) Family Member $\text{C}(\text{NH}_2)_3\text{SO}_3\text{F}$ with Ultraviolet Optical Nonlinearity. *Angew. Chem., Int. Ed.* **2020**, *59*, 15978–15981.

(22) Jin, W. Q.; Zhang, W. Y.; Tudi, A.; Wang, L. Y.; Zhou, X.; Yang, Z. H.; Pan, S. L. Fluorine-Driven Enhancement of Birefringence in the Fluorooxosulfate: A Deep Evaluation from a Joint Experimental and Computational Study. *Adv. Sci.* **2021**, 2003594.

(23) Yu, P.; Wu, L. M.; Zhou, L. J.; Chen, L. Deep-Ultraviolet Nonlinear Optical Crystals: $\text{Ba}_3\text{P}_3\text{O}_{10}\text{X}$ (X = Cl, Br). *J. Am. Chem. Soc.* **2014**, *136*, 480–487.

(24) Lu, X. F.; Chen, Z. H.; Shi, X. R.; Jing, Q.; Lee, M. H. Two Pyrophosphates with Large Birefringences and Second-Harmonic Responses as Ultraviolet Nonlinear Optical Materials. *Angew. Chem., Int. Ed.* **2020**, *59*, 17648–17656.

(25) Qi, L.; Chen, Z.; Shi, X.; Zhang, X.; Jing, Q.; Li, N.; Jiang, Z.; Zhang, B.; Lee, M. H. $\text{A}_3\text{BBi}(\text{P}_2\text{O}_7)_2$ (A = Rb, Cs; B = Pb, Ba): Isovalent Cation Substitution to Sustain Large Second-Harmonic Generation Responses. *Chem. Mater.* **2020**, *32*, 8713–8723.

(26) Ewald, B.; Huang, H.; Kniep, R. Structural Chemistry of Borophosphates, Metalloborophosphates, and Related Compounds. *Z. Anorg. Allg. Chem.* **2007**, *633*, 1517–1540.

(27) Wu, B. L.; Hu, C. L.; Tang, R. L.; Mao, F. F.; Feng, J. H.; Mao, J. G. Fluoroborophosphates: a Family of Potential Deep Ultraviolet NLO Materials. *Inorg. Chem. Front.* **2019**, *6*, 723–730.

(28) Ding, Q. R.; Zhao, S. G.; Li, L. N.; Shen, Y. G.; Shan, P.; Wu, Z. Y.; Li, X. F.; Li, Y. Q.; Liu, S.; Luo, J. H. Abrupt Structural Transformation in Asymmetric ABPO_4F (A = K, Rb, Cs). *Inorg. Chem.* **2019**, *58*, 1733–1737.

(29) Schulz, C.; Eiden, P.; Klose, P.; Ermantraut, A.; Schmidt, M.; Garsuch, A.; Krossing, I. Homoleptic Borates and Aluminates

Containing the Difluorophosphato Ligand - $[\text{M}(\text{O}_2\text{PF}_2)_x]^{x-}$ - Synthesis and Characterization. *Dalton Trans.* **2015**, *44*, 7048–7057.

(30) Connelly, N. G.; Damhus, T.; Hartshorn, R. M.; Hutton, A. T. *Nomenclature of Inorganic Chemistry*; RSC Publishing: Cambridge, 2005.

(31) Kee, J.; OK, K. M. Hydrogen-Bond-Driven Synergistically Enhanced Hyperpolarizability: Chiral Coordination Polymers with Nonpolar Structures Exhibiting Unusually Strong Second-Harmonic Generation. *Angew. Chem., Int. Ed.* **2021**, DOI: 10.1002/anie.202106812.

(32) Lu, J.; Yue, J. N.; Xiong, L.; Zhang, W. K.; Chen, L.; Wu, L. M. Uniform Alignment of Non- π -Conjugated Species Enhances Deep Ultraviolet Optical Nonlinearity. *J. Am. Chem. Soc.* **2019**, *141*, 8093–8097.

(33) Nandhini, S.; Sudhakar, K.; Muniyappan, S.; Murugakoothan, P. Systematic Discussions on Structural, Optical, Mechanical, Electrical and Its Application to NLO Devices of a Novel Semi-Organic Single Crystal: Guanidinium Tetrafluoroborate (GFB). *Opt. Laser Technol.* **2018**, *105*, 249–256.

(34) Park, J. G.; Aubrey, M. L.; Oktawiec, J.; Chakarawet, K.; Darago, L. E.; Grandjean, F.; Long, G. J.; Long, J. R. Charge Delocalization and Bulk Electronic Conductivity in the Mixed-Valence Metal-Organic Framework $\text{Fe}(1,2,3\text{-Triazolate})_2(\text{BF}_4)_x$. *J. Am. Chem. Soc.* **2018**, *140*, 8526–8534.

(35) Farina, P.; Latter, T.; Levason, W.; Reid, G. Lead(ii) Tetrafluoroborate and Hexafluorophosphate Complexes with Crown Ethers, Mixed O/S- and O/Se-Donor Macrocycles and Unusual $[\text{BF}_4]^-$ and $[\text{PF}_6]^-$ Coordination. *Dalton Trans.* **2013**, *42*, 4714–4724.

(36) Wiench, J. W.; Michon, C.; Ellern, A.; Hazendonk, P.; Iuga, A.; Angelici, R. J.; Pruski, M. Solid-State NMR Investigations of the Immobilization of a BF_4^- Salt of a Palladium(II) Complex on Silica. *J. Am. Chem. Soc.* **2009**, *131*, 11801–11810.

(37) Weil, M.; Puchberger, M.; Baran, E. J. Preparation and Characterization of Dimercury(I) Monofluorophosphate(V), $\text{Hg}_2\text{PO}_3\text{F}$: Crystal Structure, Thermal Behavior, Vibrational Spectra, and Solid-State ^{31}P and ^{19}F NMR Spectra. *Inorg. Chem.* **2004**, *43*, 8330–8335.

(38) Jantz, S. G.; van Wüllen, L.; Fischer, A.; Libowitzky, E.; Baran, E. J.; Weil, M.; Höpfe, H. A. Syntheses, Crystal Structures, NMR Spectroscopy, and Vibrational Spectroscopy of $\text{Sr}(\text{PO}_3\text{F}) \cdot \text{H}_2\text{O}$ and $\text{Sr}(\text{PO}_3\text{F})$. *Eur. J. Inorg. Chem.* **2016**, *2016*, 1121–1128.